

Needle Electrode-Based Electromechanical Reshaping of Cartilage

CYRUS T. MANUEL,^{1,3} ALLEN FOULAD,¹ DMITRIY E. PROTSENKO,¹ ALI SEPEHR,^{1,2} and BRIAN J. F. WONG^{1,2,3}

¹Beckman Laser Institute, University of California Irvine, Irvine, CA 92612, USA; ²Department of Otolaryngology, Head and Neck Surgery, University of California Irvine, Orange, CA 92868, USA; and ³Department of Biomedical Engineering, 3120 Natural Sciences II, University of California Irvine, Irvine, CA 92612, USA

(Received 27 July 2009; accepted 26 May 2010; published online 8 July 2010)

Associate Editor Sean Kohles oversaw the review of this article.

Abstract—Electromechanical reshaping (EMR) of cartilage provides an alternative to the classic surgical techniques of modifying the shape of facial cartilages. The original embodiment of EMR required surface electrodes to be in direct contact with the entire cartilage region being reshaped. This study evaluates the feasibility of using needle electrode systems for EMR of facial cartilage and evaluates the relationships between electrode configuration, voltage, and application time in effecting shape change. Flat rabbit nasal septal cartilage specimens were deformed by a jig into a 90° bend, while a constant electric voltage was applied to needle electrodes that were inserted into the cartilage. The electrode configuration, voltage (0–7.5 V), and application time (1–9 min) were varied systematically to create the most effective shape change. Electric current and temperature were measured during voltage application, and the resulting specimen shape was assessed in terms of retained bend angle. In order to demonstrate the clinical feasibility of EMR, the most effective and practical settings from the septal cartilage experimentation were used to reshape intact rabbit and pig ears *ex vivo*. Cell viability of the cartilage after EMR was determined using confocal microscopy in conjunction with a live/dead assay. Overall, cartilage reshaping increased with increased voltage and increased application time. For all electrode configurations and application times tested, heat generation was negligible (<1 °C) up to 6 V. At 6 V, with the most effective electrode configuration, the bend angle began to significantly increase after 2 min of application time and began to plateau above 5 min. As a function of voltage at 2 min of application time, significant reshaping occurred at and above 5 V, with no significant increase in the bend angle between 6 and 7.5 V. In conclusion, electromechanical reshaping of cartilage grafts and intact ears can be effectively performed with negligible temperature elevation and spatially limited cell injury using needle electrodes.

Keywords—Electrochemistry, Cartilage, Tissue reshaping, Shape change, Reconstructive surgery, Otolaryngology, Plastic surgery.

Address correspondence to Brian J. F. Wong, Beckman Laser Institute, University of California Irvine, Irvine, CA 92612, USA. Electronic mail: cmanuel@uci.edu, bjwong@uci.edu

INTRODUCTION

Cartilage provides the framework for the aesthetic structures of the face and has multiple functions, including the maintenance of airway patency, phonation, and joint movement. The structural and aesthetic defects resulting from trauma, cancer, or congenital malformations have led to the development of surgical techniques to reshape cartilage to recreate damaged or absent structures. Classical surgical maneuvers to reshape the cartilaginous frameworks of the face include cutting, scoring, suturing, and morselizing in an attempt to balance the intrinsic elastic forces within the tissue that would otherwise resist deformation.^{1,2}

It is beneficial to avoid open surgery and general anesthesia when possible to minimize resource utilization and trauma to the patient. Open surgery has disadvantages including cost, blood loss, recovery time, scarring, and the risk of surgical and anesthetic complications. Hence, minimally invasive techniques that reshape cartilage to desired specifications are favored. Although cutting, suturing, and morselizing of cartilage for facial reconstruction have been heavily relied on for centuries, these techniques rely on open surgery and do not take advantage of the inherent property of cartilage as a charged viscoelastic hydrogel.

We have previously developed a technique to reshape cartilage, which we refer to as electromechanical reshaping (EMR).⁷ In order to perform EMR, a cartilage specimen of interest is mechanically deformed to the desired shape, while electrodes are placed in contact with the tissue and a voltage is applied. Although the exact mechanism is unknown, EMR does not depend on resistive heating for shape change and, therefore, eliminates the potential of heat associated protein denaturation and cell death.^{7,14} However, a limitation of prior EMR studies is the use of surface electrodes that must directly contact the entire

cartilage region undergoing reshaping. The use of surface electrodes is not easily reconciled with minimally invasive techniques since cutting of the skin is required to expose the cartilage. Furthermore, these electrodes are impractical for complex cartilage shapes and also expose a large area of cartilage to the effects of the applied voltage. In contrast to surface electrodes, needle electrodes are not hampered by such disadvantages.^{15–19} The purpose of this study is to determine the effects of needle electrode-based EMR on cartilage shape change using *ex vivo* rabbit and porcine models. Specifically, we aim to describe the relationships between electrode configuration, voltage, and application time in effecting shape change.

METHODS

Tissue Specimens

EMR was evaluated in rabbit nasal septal cartilage tissue ($n = 200$) as a starting point to optimize needle electrode configuration and electrical dosimetry (voltage and application time) for effective shape change. The dimensions and material properties of rabbit septal cartilage are highly consistent from animal to animal and facilitate large-scale studies.²⁰ Nasal septa were extracted from the crania of freshly euthanized New Zealand white rabbits (9–12 weeks old) obtained from a local abattoir.²⁰ Septa were then cut into $20 \pm 0.5 \text{ mm} \times 5 \pm 0.2 \text{ mm}$ sections and stored in normal saline in a cold room at $4 \text{ }^\circ\text{C}$ until needed for use ($< 24 \text{ h}$).

In order to evaluate the clinical feasibility of needle-based EMR for use in reshaping the ear, freshly harvested rabbit ($n = 5$) and porcine ($n = 5$) auricles were reshaped using the most effective and practical settings derived from the septal cartilage experimentation. In both species, the pinna from the base of the bony external auditory canal to the tip was excised intact. Hair was not removed. All pinnae were rinsed with normal saline solution to remove dirt and other debris.

Experimental Setup

A schematic that describes the general embodiment of the needle EMR process is illustrated in Fig. 1a. In order to perform EMR, the cartilage specimen was compressed between the two parts of a foam rubber jig to bend the specimen into a 90° angle. While the cartilage was held in deformation, needle electrodes were inserted through the jig and through the entire thickness of the specimen. Preliminary study with stainless steel hypodermic needles resulted in deposits of metallic redox byproducts that were observed at the

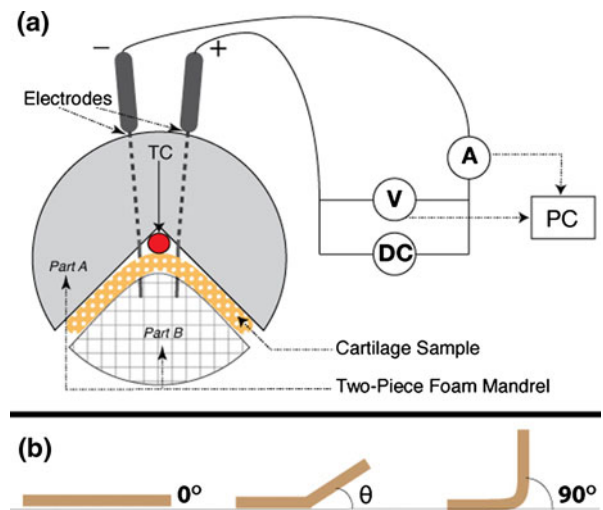


FIGURE 1. (a) Schematic diagram of the cartilage reshaping apparatus. TC indicates location of thermocouple. (b) Measurement of bend angle, θ .

needle insertion sites. Therefore, the whole experimentation was performed with passivated platinum needles (F-E2M-48, Grass Technologies, West Warwick, RI). The platinum needles were connected to the appropriate leads of a DC power supply (E3646A, Agilent Technologies, Inc, Palo Alto, CA). In order to measure tissue temperature, a small thermocouple was placed in contact with the specimen between the jig and the apex of the bend. A custom program (LabVIEW, National Instruments, Austin, TX) running on a computer workstation was used to operate the power supply to control voltage and application time, and to record current flow between the electrodes. After EMR, all the samples were left in the jig under continued deformation for 1 min with no voltage application. The bent specimen was then removed from the jig and left undisturbed without deformation for an additional minute. The specimen was then photographed using a digital camera (Digimax i5, Samsung, Ridgefield Park, NJ). The bend angle was determined for each photograph using the protractor function in ImageJ (National Institute of Health, Rockville, MD).

Analysis of Bend Angles

The bend angle of the reshaped specimens can range from 0° to 90° . Native flat septa, for example, will have bend angle of 0° , whereas the theoretical maximum bend angle using the jig is 90° (Fig. 1b). A smaller bend angle correlates with a greater degree of reversion to the original shape, and indicates a less efficacious EMR setting. Statistical analysis was performed on measured bend angles using one-way general linear model analysis of variance (ANOVA) for the calculation of the

means of EMR dosimetry differences. When significant effects of EMR modification were detected by ANOVA, a paired t test was performed to determine which voltage and time sets exhibited statistically significant results ($p < 0.05$).

Septal Cartilage EMR Settings: Electrode Configuration, Voltage, and Time

Computer models were created and solved with a finite element analysis package (COMSOL Multiphysics, COMSOL, Palo Alto, CA) to visualize the spatial distribution of electric potential and electric field. Four electrode configurations consisting of either 2, 4, or 8 needles were tested systematically (Fig. 2). The simplest electrode configuration consisted of one anode and one cathode separated by a distance of 2 mm (Fig. 2a). The electrodes were positioned so that

the apex of the bend formed by the jig was centered between the anode and cathode. Two other configurations consisted of an electrode placed at each of the four corners of an imaginary 2 mm \times 2 mm square that is centered at the apex of the bend. The two configurations differed by the arrangement of electrode polarity (Figs. 2b and 2c). The last configuration consisted of eight electrodes. In this configuration, a cathode was placed at the four corners of a 2 mm \times 2 mm square, and an anode was placed 3 mm lateral to each cathode (Fig. 2d).

The effect of voltage and application time on shape change was examined for each of the four electrode configurations. Voltage and application time were varied systematically from 0 to 10 V with 2.5 V increment and from 1 to 9 min with 1 min increment, respectively. A voltage of 10 V generated significant heat ($>5^\circ\text{C}$ after 2 min) and was eliminated from further examination. Furthermore, after analysis of the results, it was reasoned that investigation of 6 V would be beneficial, and thus this voltage was also tested.

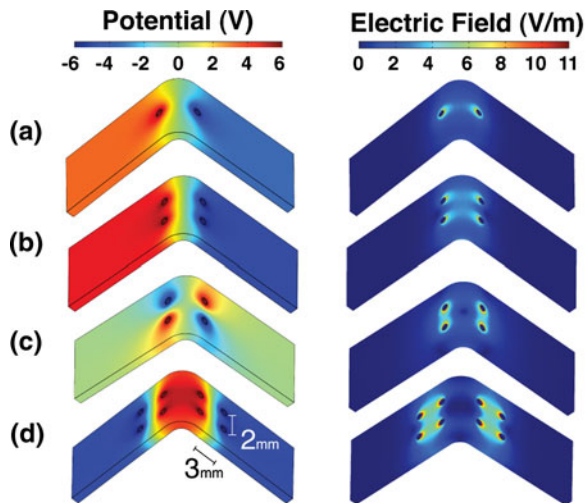


FIGURE 2. Investigated electrode geometries and their respective electric field at 6 V. (a) Two-needle electrode geometry. (b and c) Four-needle electrode geometries. (d) Eight-needle geometry.

Clinical Feasibility Experiments: EMR of Intact Rabbit and Porcine Ears

The results of septal cartilage experiments guided the selection of the electrode configuration and EMR dosimetry for the reshaping of intact rabbit and porcine ears. Both species of ears were folded along a line perpendicular to the longest axis of the ear at a distance two thirds from the base of the ear (Fig. 3a). For the rabbit ears, a jig to maintain a 90° bend during EMR and an eight-electrode configuration employing 6 V for 2 min was used as described for the septal cartilage reshaping studies. However, due to the relatively large thickness and the greater resistance to deformation of porcine ears, a clamp was used to completely fold the porcine ears in a 180° bend as opposed to the 90° bend of rabbit ears (Fig. 3b). Furthermore, the application time was increased to

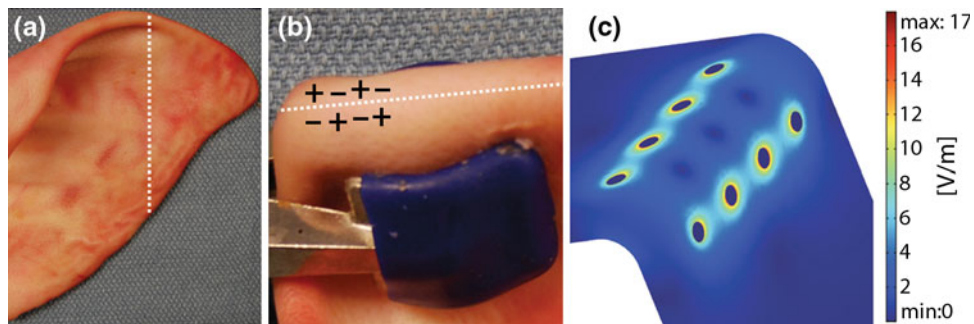


FIGURE 3. Reshaping of porcine ear. (a) Specimen before EMR. Dotted line indicates the region of flexure. (b) Electrode geometry along apex of bent ear. (c) Computer model of the tangential electric field at 6 V.

5 min for porcine ears. In addition, a slightly modified version of the eight-electrode configuration was used for porcine ears (Figs. 3b and 3c). In this updated configuration, two rows of four electrodes were separated by a distance of 3 mm with the center of this distance at the apex of the bend. Within each row, the electrodes were staggered in polarity and separated by a distance of 2 mm.

Both species of ears were electromechanically reshaped segment by segment in 1-cm intervals. After reshaping a 1-cm segment, the jig was left in place without voltage application for 1 min. The needles were then removed, and the jig was shifted along the bend to deform a new 1-cm section of ear adjacent to the recently modified region. The EMR process was repeated sequentially until the total width of the ear was modified. The ears were then photographed, and the bend angle was calculated as described for the septal reshaping studies. In addition, the completely reshaped ears were flexed with a thumb and forefinger to perform a subjective assessment of overall mechanical behavior. The surfaces of the ear at the electrode penetration sites were examined for signs of tissue injury.

Cell Viability Analysis

A cell viability assay system combined with fluorescent confocal microscopy was performed as described by Choi and coworkers to determine the degree of injury generated around the electrodes in the reshaped rabbit and porcine ears.^{3,4,8,10} A cross-sectional slice was cut lengthwise through the center of electrode insertion sites 1 h after EMR. The tissue was then stained using a LIVE/DEAD[®] cell viability assay (Molecular Probes, Eugene, OR), and the distribution of live and dead cells was visualized with a confocal microscope (LSM 510 META, Carl Zeiss, Jena, Germany).

RESULTS

Qualitative Assessment of Rabbit Septal Tissue After EMR

In accordance with prior study, gas formation (via hydrolysis of water) occurred at each electrode and appeared to increase in intensity with voltage.¹⁴ A small circular region of tissue (diameter <2 mm) surrounding the anode (+) needle electrodes appeared to be more transparent and softer immediately after EMR. In contrast, the tissue surrounding the cathode (-) electrodes was slightly more opaque than native cartilage tissue. When experimental specimens were

manually flexed in the direction opposite to the created bend, they had adequate memory to return to their reshaped geometry.

Electrode Configuration

For any given voltage and time combination, the eight-needle electrode configuration produced the highest bend angle while the two-needle electrode configuration produced non-significant reshaping. Both of the four-needle electrode configurations produced bend angles that were significantly lower than the angles obtained with the eight-needle electrode configuration. There was no significant difference between the two polarity patterns of the four-needle configurations.

Reshaping of Rabbit Septum

Considering the efficacy of the eight-needle configuration, the subsequent analysis of voltage and application time focuses on this electrode arrangement.

Regardless of application time (1–9 min), EMR using 2.5 V produced no significant shape change compared to the control. Voltages above 2.5 V (5, 6, and 7.5 V) produced significant shape change that increased with increase in application time. Figure 4 is a photographic montage illustrating the increase in shape change of rabbit septa as application time was increased using 6 V and the eight-needle electrode

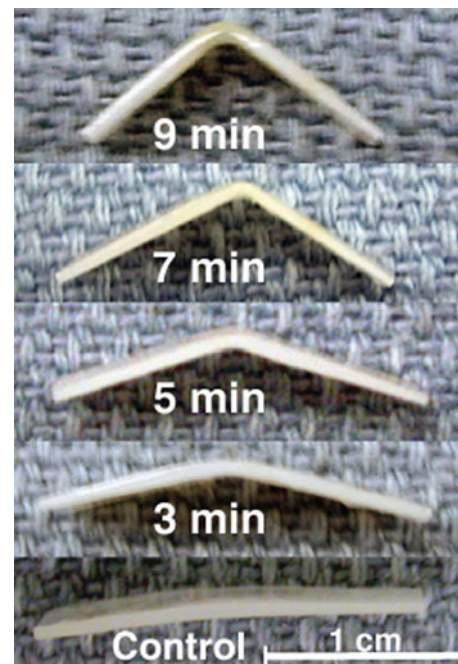


FIGURE 4. Reshaped rabbit septa using 6 V.

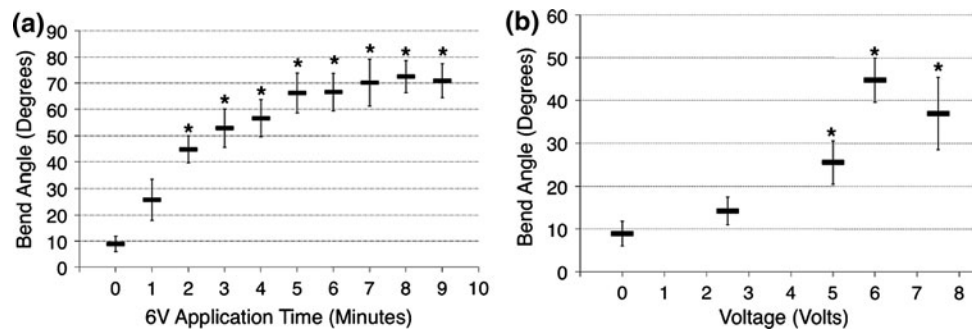


FIGURE 5. Shape retention after EMR with the eight-needle configuration. (a) Time dependent reshaping of rabbit nasal septa using 6 V. (b) Voltage dependent reshaping of rabbit nasal septa using 2 min of application time. Data are mean \pm SD, $n = 4$. * Significant difference with comparison to control ($p < 0.05$).

configuration. Figure 5a further demonstrates shape retention as a function of application time at 6 V. There is an observed trend that the bend angle increases with increasing application time and begins to plateau at approximately 5 min. Reshaping with an application time of 1 min was not significantly different from the control; however, all the application times from 2 to 9 min resulted in bend angles that were significantly greater than the control ($p < 0.05$). The shortest application time that produced a statistically greater shape change than an application time of 2 min was an application time of 8 min ($p < 0.05$).

Retained bend angle as a function of voltage for an application time of 2 min using the eight-electrode geometry is shown in Fig. 5b. Reshaping at 2.5 V was not significantly different from the control; however, at 5, 6, and 7.5 V, they were more significant than the control ($p < 0.05$). At 6 V, the shape change was significantly greater than at 2.5 V ($p < 0.05$). There was no significant difference in shape change between 6 and 7.5 V and between 6 and 5 V.

The maximal change in surface temperature during EMR was negligible ($< 1^\circ\text{C}$) at and below 6 V for all application times up to 9 min. At 7.5 V, surface temperature approached approximately 2.4°C at 2 min, and significantly increased to approximately 9.5°C at 9 min.

Figure 6 demonstrates electric current evolution during the first 2 min of reshaping using the experimental voltages. Current amplitude increased with increase in voltage. For all voltages, the electric current declined slightly during first 2–3 s of voltage application. Following this initial interval, the current evolution depended on the applied voltage. At 2.5 and 5 V, the current was nearly constant during the remainder of the 2 min interval. At 6 V, there was a rise in current which peaked at approximately 40 s, and then a decline in current. At 7.5 V, there was a much more rapid rise in current with an earlier peak at approximately 30 s, followed by a more rapid decline in current.

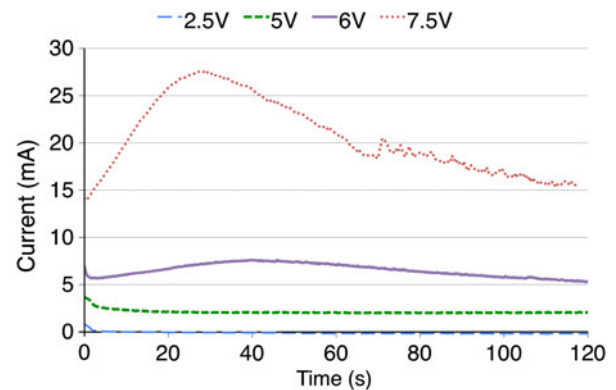


FIGURE 6. Electric current evolutions for the experimental voltages in rabbit septal cartilage during the first 2 min of EMR using the eight-needle electrode configuration.

Reshaped Intact Rabbit and Pig Ears

EMR of rabbit and porcine ears produced a sustained bend in the ears (Fig. 7). Compared to rabbit ears, porcine ears required a greater than 90° bend during EMR and an increase in application time to counter the native shape memory effect. The ears maintained the induced bend along the cathode insertion points and retained this deformation even after manually straightening the specimen. The EMR process affected only a small area (< 1 mm diameter) of skin surrounding the electrodes, which showed evidence of dehydration (Figs. 7c and 7f). It is important to note that the needles were not insulated in contact points with skin.

Cell Viability

Viability analysis using confocal microscopy identified live (green) and dead (red) cells in cross-sectional slices of cartilage that underwent EMR (Fig. 8). In Fig. 8a, rabbit auricular cartilage (0.2-mm thickness) reshaped using an applied voltage of 6 V for 2 min

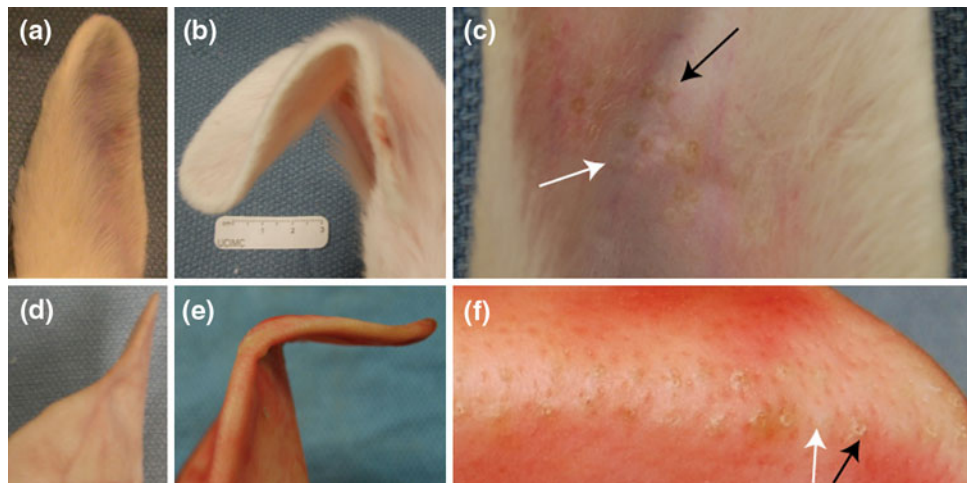


FIGURE 7. EMR of rabbit and pig ear. (a) Rabbit ear control. (b) Rabbit ear after EMR. (c) Electrode insertion points in reshaped rabbit ear. The white arrow points to the region of prior anode insertion and the black arrow points to the region of prior cathode insertion. (d) Pig ear control. (e) Pig ear after EMR. (f) Electrode insertion points in reshaped pig ear.

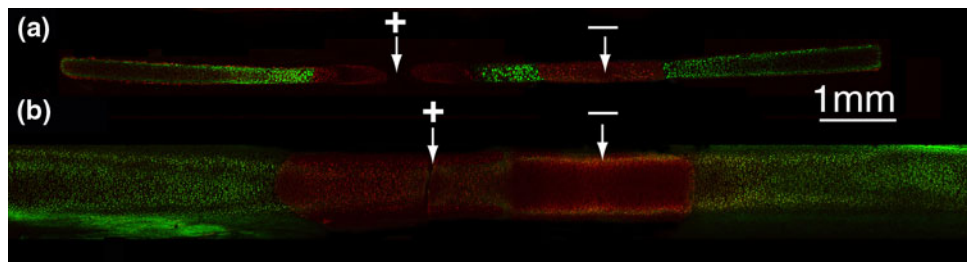


FIGURE 8. Confocal images of reshaped cartilage cross-sections stained using live/dead assay. Arrows indicate insertion points. (a) Rabbit auricular cartilage after EMR using 6 V for 2 min. (b) Porcine auricular cartilage after EMR using 6 V for 5 min.

demonstrates cell injury extending 1.1 mm away from each electrode, with viable cells between the electrodes. In Fig. 8b, porcine auricular cartilage (0.8-mm thickness) reshaped using an applied voltage of 6 V for 5 min demonstrates cell injury extending 2 mm away from each electrode.

DISCUSSION

This study aimed to determine the feasibility of using needle-based EMR to reshape cartilage. We identified a set of voltage and time parameters for effective shape change in both septal cartilage grafts as well as in intact *ex vivo* auricular specimens. Future studies aimed at moving this technology toward clinical implementation will need to further optimize electrical dosimetry parameters and electrode configurations, ideally using an *in vivo* model, as the effort herein was largely empirical. As with most reshaping methods in living tissue, shape change comes at the expense of tissue viability and balancing these competing effects is essential in the optimization process.

Needle Electrode Configuration

Needle placement is a crucial consideration and must accomplish several objectives. First, electrodes must be placed in the regions of increased internal stress caused by tissue flexure. Second, electrodes should be separated by an appropriate distance. Needles separated by too great a distance will require increased voltage to overcome the added resistance, and thus lead to increased heat production and subsequent thermal injury. However, needles placed too close to each other will increase the amount of tissue perforation and injury. Third, the arrangement of electrode polarity should be optimized because different redox reactions occur at the cathode and anode, and these reactions have profoundly different effects on tissue mechanical behavior. Anode (+) regions create local acidic regions and are generally softer after EMR, which may allow differentiated chondrocytes to easily migrate to this electrochemically modified tissue matrix and proliferate.^{6,13} Cathode (−) regions instead produce hydroxyl ions and hydrogen gas making the electrode–electrolyte interface increasingly basic as water is consumed.

Among the four experimental electrode configurations evaluated in the experimentation with septal cartilage, the eight-electrode configuration produced the greatest amount of cartilage shape change. Therefore, this electrode configuration was selected to demonstrate reshaping in intact rabbit ears. In the experiment to demonstrate reshaping in porcine ear, the eight-electrode geometry was modified so that the overall electric field was focused closer to the bend.

Reshaping Parameters: Voltage and Time

Previously, we have demonstrated a relationship between voltage and application time, such that shape change is correlated with total charge transfer.¹⁴ Thus, within limits, a decrease in application time can be offset by an increase in voltage to yield the same amount of transferred charge and thus the same degree of shape change. For example, a 45° bend can be achieved with EMR using 5 V for 5 min or using 6 V for 2 min. High voltages will potentially require less EMR time and provide for a faster clinical procedure, but will also result in high current and subsequent heat generation due to resistive heating. Another consequence of higher voltages is that there appears to be a more rapid consumption of water in the vicinity of the electrodes by redox processes. This can quickly lead to tissue dehydration and potentially greater cell injury in the vicinity of the electrodes. Applying a lower voltage for a longer application time will reduce redox reaction intensity and allow the diffusion of water from the bulk of the specimen to replace the water consumed at the electrodes.

Using rabbit septal cartilage, we determined that 6 V was the most ideal EMR setting among the dosimetries investigated using the eight-electrode configuration. EMR using 6 V produced a significantly greater amount of shape change compared to 5 V. Furthermore, an increase in the shape change observed at a voltage of 7.5 V was not significantly different from the shape change observed at 6 V, but a greater amount of heat production was observed at 7.5 V.

At 6 V, an application time ranging from 2 to 7 min yielded no significant difference in shape change. Although shape change at 8 min was significantly greater than at 2 min, the increase in shape change was modest. Therefore, to minimize reshaping time and voltage-related damage, an application time of 2 min was favored.

Evolution of Electric Current

The redox reactions at the cartilage–needle interface, which occur during voltage application facilitate the formation of an electric current in the EMR circuit.

The amplitude of the current depends on the magnitude of the applied voltage and concentration of molecules involved in the reactions. In our prior EMR experiments with surface electrodes, we observed a swift rise in current magnitude during the first 5–10 s of voltage application (2–9 V) that was followed by a steady decline in current for the remainder of the reshaping time.¹⁴ In contrast, needle-based EMR results in a nearly constant flow of current using 2.5 and 5 V for an application time of 2 min. Although there is a rise in current using 6 and 7.5 V, this rise is modest and takes a greater time to peak as compared to the electric current trend associated with surface electrodes.

Rapid consumption of molecules involved in the redox reactions at the tissue–electrode interface and the subsequent slower diffusion flux of such molecules from the tissue bulk is responsible for the characteristic rise-and-fall pattern of the electric current observed in the case of EMR with surface electrodes.¹⁴ However, the high electric field near the needle electrode produces a diffusion flux that is much stronger than the flux between surface electrodes at the same applied voltage. This strong flux might provide sufficient molecules to replace consumption of molecules in the redox reaction at the electrode interface and thus maintain a constant current at low voltages and reduce the change in current at higher voltages.

Subjective Measures

In this study, manual inspection of septal cartilage after EMR demonstrated that cartilage specimens maintain reshaping geometry and do not demonstrate significant weakening due to perforation by the electrodes or due to electrochemical tissue modifications. The qualitative assessment of the tissue mechanical properties warrants a comment. Although it is important to numerically test the mechanical properties of reshaped cartilage, this study solely focused on developing EMR toward a more clinically relevant method to incorporate needle electrodes. A detailed mechanical analysis of reshaped specimens after EMR would require complex modeling since the cartilage is anisotropic and does not compare to a simple linear tension or compression model, which is beyond the scope of this study. Furthermore, the tissues affected from each electrode polarity (anode and cathode) must be separated and tested independently because the polarity likely affects the tissue mechanical properties differently.

Ear Reshaping

EMR using needle electrodes was effective in reshaping *ex vivo* rabbit and pig ears. However, pig ears required overcorrection and a longer application

time to achieve a 90° bend. This is because pig ears are profoundly thicker than both their rabbit and human counterparts with thicker cartilage, skin, and underlying connective tissue. The cartilage thicknesses at the region of modification for the rabbit and pig ears were approximately 0.2 and 0.8 mm, respectively. This supports the use of needle-based EMR in the reshaping of human ear, because the thickness of human ear, approximately 0.6 mm, falls within the range of thicknesses investigated in our study.⁵ However, it is likely that in the clinical reshaping of human ears some degree of overcorrection will be needed, at least in areas of thicker tissue.

A clinical implementation of an “ear retainer” or moulage may facilitate and guide the tissue repair process and aid with establishing a stable shape change.¹² In addition, for surgical application, needle insulation will be necessary to protect the skin in contact with electrodes from being affected by the EMR process. This is a minor design issue that can be addressed during the development of EMR medical devices.

Cell Viability

Confocal microscopy in conjunction with a live/dead assay is a well-established method used to determine acute chondrocyte viability.^{3,4,10,11} The electrical dosimetry settings (6 V, 2 min) used for reshaping the rabbit ears resulted in a 2.2-mm diameter of cell injury that was limited to the region surrounding the electrodes. In pig ears, the application time was raised to 5 min, which resulted in a 4-mm diameter of cell injury around each electrode. Optimization of EMR dosimetry settings and needle placement can limit cell injury and intersperse the areas of tissue damage within areas of normal tissue. Furthermore, laser cartilage reshaping studies have demonstrated evidence of cartilage regeneration in regions of thermally induced cell death.^{8,9} Accordingly, viable perichondrium and chondrocytes surrounding the regions of EMR induced injury can potentially aid in the repopulation of the damaged areas with viable chondrocytes.

CONCLUSION

In this study, we proposed a method to use needle electrodes to electromechanically reshape cartilage. This is a significant departure from EMR performed using surface electrodes, which requires incisions for placement and direct contact of the electrodes with the region of cartilage being reshaped. EMR using needle electrodes resulted in shape change that increased with

both voltage and application time. Effective shape change did not involve resistive heating and was associated with spatially limited cell injury. Since needles can easily be inserted through skin and mucosa into cartilage within the ear, nose, and trachea, EMR may be amenable to minimally invasive and endoscopic techniques that may provide an alternative to current cut and suture open surgical methods.

ACKNOWLEDGMENTS

This study was supported by the Department of Defense Deployment Related Medical Research Program (DR090349). Air Force Office of Scientific Research (FA9550-04-1-0101) and the National Institutes of Health (DE019026, DC005572, DC 00170, RR 01192).

OPEN ACCESS

This article is distributed under the terms of the Creative Commons Attribution Noncommercial License which permits any noncommercial use, distribution, and reproduction in any medium, provided the original author(s) and source are credited.

REFERENCES

- ¹Adamson, P. A., and J. A. Litner. Otoplasty technique. *Otolaryngol. Clin. North Am.* 40:305–318, 2007.
- ²Adamson, P. A., B. L. McGraw, and G. J. Tropper. Otoplasty: critical review of clinical results. *Laryngoscope* 101:883–888, 1991.
- ³Chae, Y., D. Protsenko, P. K. Holden, C. Chlebicki, and B. J. Wong. Thermoforming of tracheal cartilage: viability, shape change, and mechanical behavior. *Lasers Surg. Med.* 40:550–561, 2008.
- ⁴Choi, I. S., Y. S. Chae, A. Zemek, D. E. Protsenko, and B. Wong. Viability of human septal cartilage after 1.45 micron diode laser irradiation. *Lasers Surg. Med.* 40:562–569, 2008.
- ⁵Danter, J., R. Siegert, and H. Weerda. Ultrasound measurement of skin and cartilage thickness in healthy and reconstructed ears with a 20-MHz ultrasound device. *Laryngorhinootologie* 75:91–94, 1996.
- ⁶Hall, B. K. Cartilage. New York: Academic Press, 1983.
- ⁷Ho, K. K., S. H. Diaz Valdes, D. E. Protsenko, G. Aguilar, and B. J. Wong. Electromechanical reshaping of septal cartilage. *Laryngoscope* 113:1916–1921, 2003.
- ⁸Holden, P. K., C. Chlebicki, and B. J. Wong. Minimally invasive ear reshaping with a 1450-nm diode laser using cryogen spray cooling in New Zealand white rabbits. *Arch. Facial Plast. Surg.* 11:399–404, 2009.
- ⁹Jones, N., A. Sviridov, E. Sobol, A. Omelchenko, and J. Lowe. A prospective randomised study of laser reshaping of cartilage in vivo. *Lasers Med. Sci.* 16:284–290, 2001.

- ¹⁰Karam, A. M., D. E. Protsenko, C. Li, R. Wright, L. H. Liaw, T. E. Milner, and B. J. Wong. Long-term viability and mechanical behavior following laser cartilage reshaping. *Arch. Facial Plast. Surg.* 8:105–116, 2006.
- ¹¹Li, C., D. E. Protsenko, A. Zemek, Y. S. Chae, and B. Wong. Analysis of Nd:YAG laser-mediated thermal damage in rabbit nasal septal cartilage. *Lasers Surg. Med.* 39:451–457, 2007.
- ¹²Mordon, S., T. Wang, L. Fleurisse, and C. Creusy. Laser cartilage reshaping in an in vivo rabbit model using a 1.54 μm Er:Glass laser. *Lasers Surg. Med.* 34:315–322, 2004.
- ¹³Nogami, H., H. Aoki, T. Okagawa, and K. Mimatsu. Effects of electric current on chondrogenesis in vitro. *Clin. Orthop. Relat. Res.* 163:243–247, 1982.
- ¹⁴Protsenko, D. E., K. Ho, and B. J. Wong. Stress relaxation in porcine septal cartilage during electro-mechanical reshaping: mechanical and electrical responses. *Ann. Biomed. Eng.* 34:455–464, 2006.
- ¹⁵Rhim, H., H. K. Lim, Y. S. Kim, and D. Choi. Percutaneous radiofrequency ablation with artificial ascites for hepatocellular carcinoma in the hepatic dome: initial experience. *AJR Am. J. Roentgenol.* 190:91–98, 2008.
- ¹⁶Stuck, B. A., A. Sauter, K. Hormann, T. Verse, and J. T. Maurer. Radiofrequency surgery of the soft palate in the treatment of snoring. A placebo-controlled trial. *Sleep* 28:847–850, 2005.
- ¹⁷Utley, D. S., R. L. Goode, and L. Hakim. Radiofrequency energy tissue ablation for the treatment of nasal obstruction secondary to turbinate hypertrophy. *Laryngoscope* 109:683–686, 1999.
- ¹⁸van den Bosch, M., B. Daniel, V. Rieke, K. Butts-Pauly, E. Kermit, and S. Jeffrey. MRI-guided radiofrequency ablation of breast cancer: preliminary clinical experience. *J. Magn. Reson. Imaging* 27:204–208, 2008.
- ¹⁹Vlastos, G., and H. M. Verkooijen. Minimally invasive approaches for diagnosis and treatment of early-stage breast cancer. *Oncologist* 12:1–10, 2007.
- ²⁰Wong, B. J., K. K. Chao, H. K. Kim, E. A. Chu, X. Dao, M. Gaon, C. H. Sun, and J. S. Nelson. The porcine and lagomorph septal cartilages: models for tissue engineering and morphologic cartilage research. *Am. J. Rhinol.* 15:109–116, 2001.